Real-time on-board condition monitoring of train axle bearings

I Corni[1,2], N Symonds[1], R J K Wood[1], A Wasenczuk[2], D Vincent[2]
[1] National Centre for Advanced tribology at Southampton, Faculty of Engineering and the Environment, University of Southampton, UK
[2] Perpetuum Ltd, Southampton, UK

ABSTRACT

Premature failure of rail axle bearings causes a significant increase in train operating costs and can impact train safety. A new on-board condition monitoring approach provided by Perpetuum Ltd is fitted on passenger trains to provide the operator with real-time information on bearing health. This new technology allows the detection of early bearing damage.

This paper reports an initial study to understand the source of vibrations. The final aim of the project is to connect the increasing vibration data to the bearing surface damage, measured with surface profilometry.

1 INTRODUCTION

Rolling element bearings are mechanical components widely employed in industrial applications, from rotating machinery to means of transport. Rolling element bearings consist of a complex structure (outer ring, inner ring, cage and rollers) and usually operate in harsh working environments (e.g. high temperature, rotational speed and loads) and therefore they are often at risk of failure.

Fatigue is the normal failure mode for bearings that are properly installed and maintained. Unfortunately, numerous bearings suffer early failures due to poor fitting, insufficient lubrication, overloading, overheating, contamination, unbalance and misalignment. Early failure can cause the breakdown of the machinery, decrease its efficiency and even reduce safety with risks to lives (1-3). For these reasons it is vital to monitor the bearing condition and lots of research has been recently undertaken in fault diagnosis using mainly vibrations (4-14), but also acoustic emissions (15-16) and temperature measurements. Changes in vibration signature have been employed for many years to detect degrading bearings before failure; but often the bearing vibrations cannot be directly measured because they are affected by vibrations from other parts of the apparatus (background noise) making condition monitoring more complex (3). In order to overcome this difficulty, numerous signal processing techniques (e.g. envelope spectrum analysis (10, 17), empirical mode decomposition (EMD) (2, 7, 8, 10, 18-19), Hilbert-Huang transform (HHT) (4, 7), wavelet transform (WT) (5, 12, 20) and minimum entropy deconvolution (MED) (17)) have been developed to identify fault characteristics precisely in the vibration data. The data used to develop these techniques were partly originated in the laboratory (1, 4, 6, 8, 10-14, 19), partly obtained from the Case Western Reserve University (CWRU) bearing data centre (6-7, 21-24) and only a few acquired from in-situ equipment (i.e. mining machines (18),

servomotors running arbitrary motion profiles (9), helicopters (25-27) and traction fans (28)).

Train axle bearings are key elements in the integrity of railway wheel sets; ensuring their good condition is fundamental for train safety and this can be achieved using condition monitoring. The most common failure in axle bearings is due to rolling contact fatigue (RCF) of the outer race (29-30). Subsurface networks of cracks develop in the rolling direction by shear stresses and then deviate towards the surface causing macropits that represent a measurable surface damage (31-33).

This paper presents an initial study to correlate vibration data with bearing damage. Real-life vibration data are measured using wireless sensor nodes (WSNs) developed by Perpetuum Ltd and fitted to Southeastern operated rolling stock. This new technology monitors in real-time the vibrations of axle-bearings and successfully detects early bearing failures. The failed bearings are characterised by measuring the surface profile of the rolling area of the outer race.

2 CURRENT TECHNOLOGY

The degradation of axle bearings occurs with an increase in noise and vibration, followed by temperature (34). Nowadays, the increase in temperature is detected by trackside Hot Axle Box Detectors (HABDs); when the temperature increases the train has to be stopped immediately causing disruption to passengers and railway traffic. Therefore more research to detect precursors to run-away thermal failure using noise and vibrations has been carried out and it is still needed.

In the past 10 years technology employing noise has been developed; noise is generally detected using acoustic monitors that use the frequency of the sound to determine the damaged component (e.g. damaged bearing, noises from flanging, wheel flat, gearbox noises). Tsukahara *et al*. (34) compared the ability of two different Acoustic Bearing Detectors (ABD) (RailBAM and unknown) to detect eight faulty bearings installed on a French TGV; after 57 runs at speed between 15 and 130 km/h both ABDs located correctly 7 bearings out of 8. In the USA train axle bearings are monitored using TTCI Trackside Acoustic Detection System (TADS®) that identifies defects before overheating (35).

Due to the complexity of the train system not much research has been reported on condition monitoring of train axle bearings using vibrations. SKF Multilog online system consists of numerous modular sensors which monitor and transmit many bogie operating conditions (temperature and vibrations are measured for bearings). Laboratory experiments on 43 bearings with or without damage (previously operating on trains or artificially damaged) were carried out using train operational conditions; “good” bearings could be successfully distinguished from damaged bearings (36). Deutsche Bahn Systemtechnik has developed an on board bogie diagnostic system made of two units: the bogie-instrumentation with sensors (noise and vibration) and cables running to the diagnostic unit under the passenger’s seat. This technology can successfully detect early bearing damage (37). Moreover, Bellaj *et al*. (38) compared results from track-side ABD and on-board vibration measurements for a high speed TGV fitted with eight faulty bearings. The on-board system showed increased vibration for damaged bearings and effectively detected faulty bearings for speed higher than 60 km/h. The track-side detector revealed 75% of failed bearings using multiple runs and speed higher than 60 km/h. Currently, none of these technologies show the ability to link the level of damage to a measurable parameter.

Perpetuum Ltd has developed a new on-board system for measuring local vibrations using wireless sensor nodes (WSNs). The system is fitted on several networks in the UK, but the current work concerns Southeastern trains. The on-board self-powered WSNs are bolted onto the bearing axle housing of the Southeastern Electrostar fleet (148 trains and 4,944 wheels) covering 540 miles of tracks in the south-east of England (Figure 1). All the wheels of all the trains are individually monitored during normal passenger service.

Figure 1 – Map of the south east of England. Track covered by Southeastern trains is indicated in blue and orange; the track Tonbridge to Ashford International is in orange.

The WSN measures vibrations using a tri-axial accelerometer; the acceleration data are recorded for 4 seconds every 3 minutes. The sensor records 16,000 points per second on each axis (x is the vertical direction, y is the direction of travel and z is the direction parallel to the axle); in 4 s of recording time 192,000 points are recorded. These data points (raw data) are used to calculate: *rms X*, *rms Y*, *rms Z*, *peak X*, *peak Y, peak Z* and vertical Fast Fourier Transforms (FFTs). These data combined with train number, wheel position, date and time, speed of the train, GPS location, direction of travel, temperature, bearing health index (BHI), wheel health index (WHI) are wirelessly sent to the Cloud and are available in real-time via a website. BHI and WHI values are calculated with complex algorithms. Depending on the daily mileage of the train an average of 300-400 data are received from each WSN.

The train operator has real-time access to BHI and WHI values and uses these to identify bearing and wheel issues, respectively.

3 METHODOLOGY

The vibration data are analysed with two aims:

a) Understand the sources of the vibrations;
b) Link the increasing vibrations to the condition of the removed bearings.

Part a) requires looking at large data sets from many “good” bearings travelling at different speeds and locations. Part b) is a larger task, beyond the scope of this paper, however two example bearings are shown to demonstrate the methods and techniques being used to look at the possible relationships between vibration data and the extent of bearing damage.

In the current commercial system, the faulty bearings are identified by increasing BHI values compared to what is considered normal. In this study, the data have been re-analysed comparing the vibrations of the failed bearing with the background vibrations of the other bearings on the same train covering the same track and subjected to the same speed profiles and loadings. This method clearly identifies the extra vibrations related to the damage.

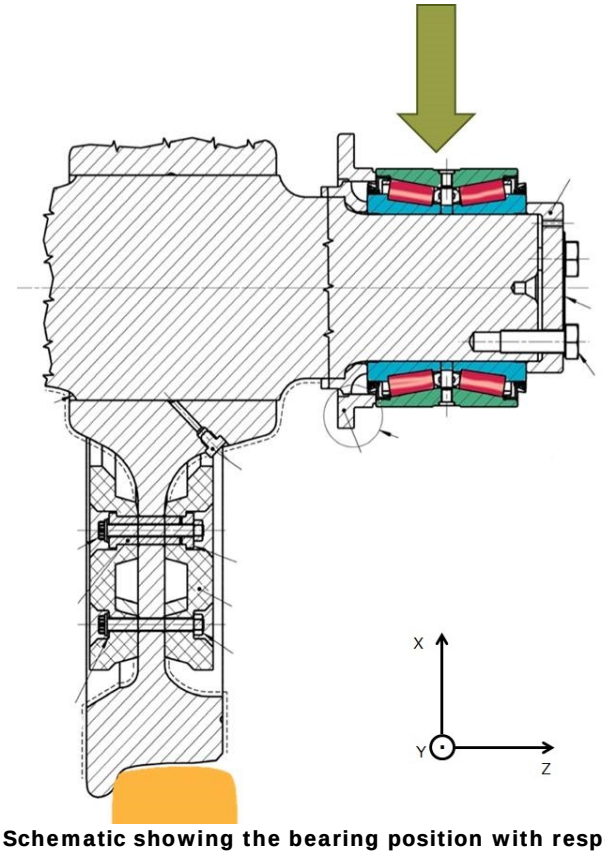

Figure 2 – Schematic showing the bearing position with respect to wheel, axle and rail.

For the purpose of this study, rms X is the parameter chosen to compare the vibrations. The vibration in X is solely affected by the loaded contact bearing-wheel-rail, as shown in Figure 2. Rms X is therefore influenced also by wheel damage. It has been confirmed that the bearings analysed are characterised only by high BHI values (and not by high WHI) confirming that the extra vibrations are only due to damage in the bearings.

Bearings with high BHI readings were removed by the operator and stripped at the Southeastern Ramsgate Maintenance depot. The bearings were then sent to the

University of Southampton for further analysis. All the bearings detected with high BHI values presented outer race damage.

The surface profile of the damaged outer race is measured at Taylor Hobson Limited (Leicester, UK) using a Talyrond 595. The bearing is positioned on a spindle top and five traces of the whole rolling area are measured with high data density (72,000 points over 360°). The traces are 10 mm apart as shown in Figure 3. The 0 mm trace is carried out outside the worn area and is used as a reference.

The volume missing on the outer race was measured using an Alicona Infinite Focus (Sevenoaks, UK), an optical non-contact profilometer. The scan was carried out using a horizontal resolution of 13.98 µm and a vertical resolution of 2.40 µm.

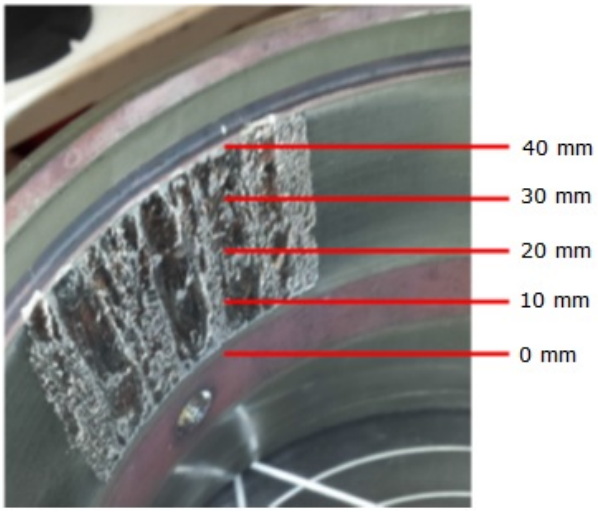

Figure 3 - Bearing outer race with position of the 5 traces measured by Talyrond 595.

4 RESULTS AND DISCUSSIONS

4.1 Factors affecting vibrations

By analysing data from numerous trains recorded during 10 months it emerged that a common vibration pattern for healthy wheels and bearings is the one shown in Figure 4. Figure 4 shows the vibrations in X, Y and Z for one wheel of one train travelling for one month all around the Southeastern train track (blue and orange track in Figure 1). This clearly demonstrates that the vibrations vary significantly in value from point to point. The vibration values change continuously but they are reproducible over time and therefore they could be used to map the railway line to check for changes in the infrastructure.

The changes in vibrations can be explained considering that the system bearing-wheel-axle-track (Figure 2) is a dynamically complex system with numerous variables affecting its behaviour. The vibrations are affected by:

- train track (e.g. fish plates, track points, junctions between tracks),
- wheel conditions,
- bearing conditions,
- loading,
- train speed and
- time (e.g. track conditions can change with time).

For this work, in order to be able to compare the vibrations of bearings from different trains; the data was filtered to eliminate most of these factors.
From the GPS data recorded, it is known that each train covers the whole Southeastern track (blue and orange in Figure 1) in a period between 2 and 6 weeks; therefore some of the factors affecting vibrations can be eliminated by using data from only one part of the track. The track *Tonbridge to Ashford International* (latitude: 51.1478 to 51.1927, longitude: 0.2639 to 0.8591 and heading: 86 to 116) (orange in Figure 1) has been chosen because: being a predominantly straight track (approximately 40 km long) there are no extra vibrations due to curves (extra load on wheels during turning) and the data are easily plotted using latitude or longitude. In a position detected by GPS there are at least 2 tracks (each track consists of two rails) going in opposite directions; only one direction (from Tonbridge to Ashford International) and only one rail (only one side of the train) are considered so that the contact rail-wheel is consistent and reproducible (this eliminates the effect of *train track*). The effect of time can be eliminated by comparing the faulty bearing with only the remaining "good" bearings on the same side of the train.

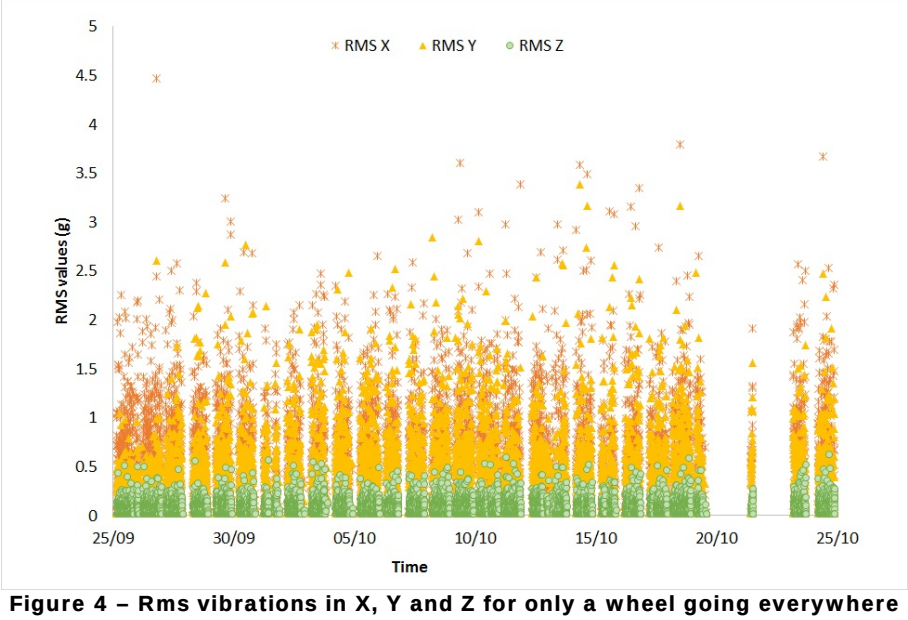

Figure 4 – Rms vibrations in X, Y and Z for only a wheel going everywhere on the train track over a month (6,900 data in each direction).

Comparing the variation of rms X (Figure 5a) and speed (Figure 5b) for the same part of the track, it is clear that the vibrations in X increase with train speed. Figure 5 shows data from 210 journeys from Tonbridge to Ashford International; the journeys are clearly repetitive with 5 stops (slow journeys) and the same speed variation. The few data from fast journeys have been eliminated. Therefore it could be concluded that generally trains run journeys with similar speed profiles on the same part of the track (e.g. same number of stops, same speed due to speed limits). Therefore it is possible to affirm that all the trains pass on a particular part of track always at the same speed (Figure 5b).

The *effect of speed* could be eliminated by using only one particular speed, but this has not been done because it would markedly decrease the number of points making comparison between different bearings very difficult.

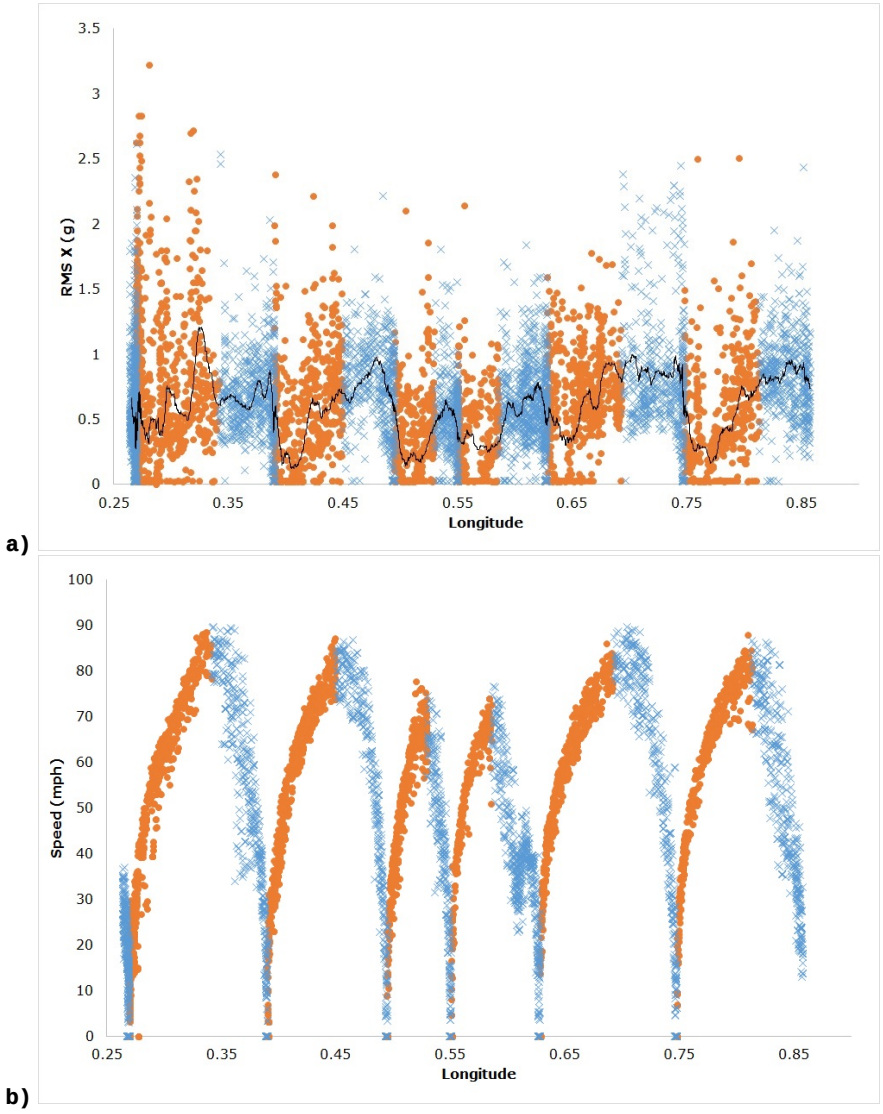

Figure 5 – a) vibration profile vs longitude (the black line shows the average vibration) and b) speed profile vs longitude for journeys of one train in a 3 month period going from Tonbridge to Ashford International (left to right). The data in orange represent accelerating time and those in blue decelerating and braking.

4.2 Vibrations of failed bearings

By comparing data from four trains travelling from Tonbridge to Ashford International during the same 2-month period it has been demonstrated that all the 16 wheels from the same side of the train have the same baseline vibrations (when they are in good health) independently from the position along the train and from the train type (results not shown here). It is therefore possible to compare the vibrations of a damaged bearing with a *baseline vibration* characteristic for the same train, journey and period of time (data from 15 WSNs). Figure 6 shows two examples of this comparison.

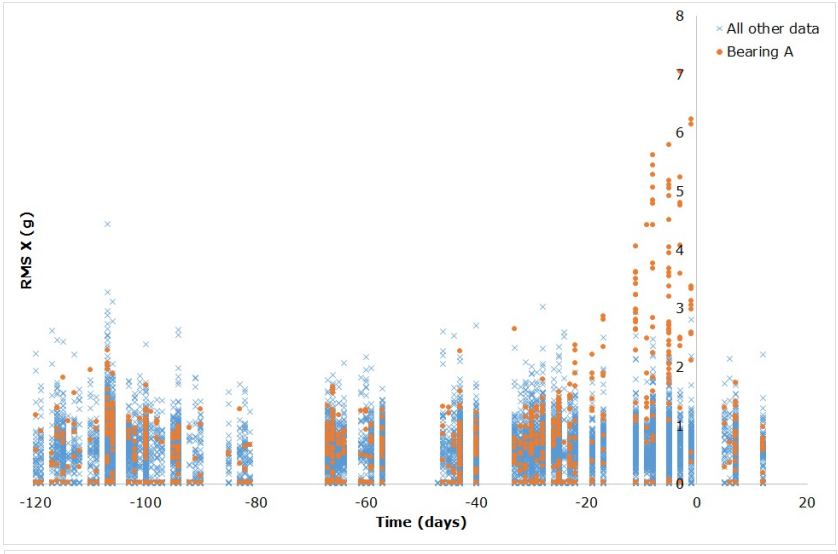

a)

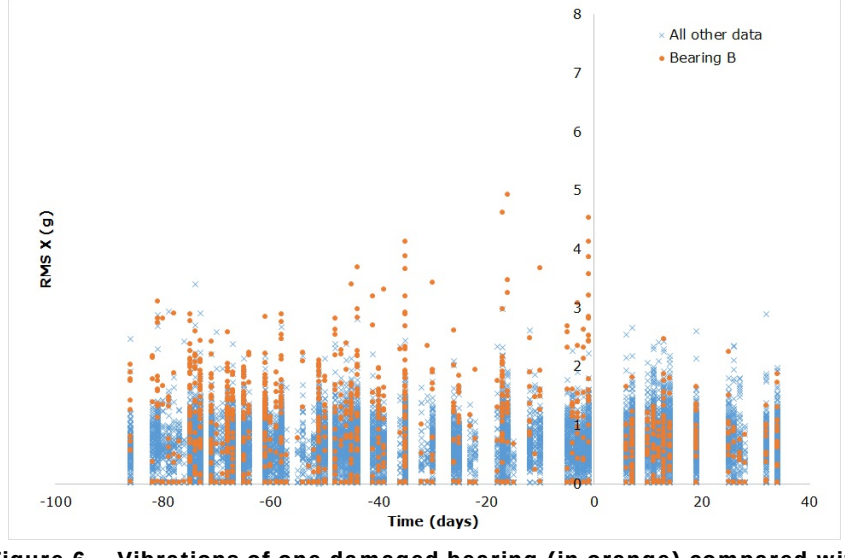

b)

Figure 6 – Vibrations of one damaged bearing (in orange) compared with the baseline vibrations of the other bearings on the same side of the same train for the same journeys and the same period of time for a) bearing A and b) bearing B. Day 0 corresponds to bearing removal.

For bearing A the vibration is very similar to the baseline vibrations until 11 days before bearing removal when the increase is very rapid. Rms X increases from 3 g to 7 g in 11 days. For bearing B the vibrations start to behave differently from the baseline 48 days before bearing removal and the increase is slow. The rms X value for this second bearing reaches only 5 g; rms X increases from 3 g to 5 g in 48 days. The vibrations of both WSNs decrease considerably after new bearings were fitted, further confirming that the excess vibrations were due only to the damage in the bearings.

Figure 7 compares the last 1,600 miles of both damaged bearings: the mean values of rms X are higher for bearing A than bearing B. During the last 400 miles bearing A displayed a mean rms X value 1.7 times greater than bearing B.

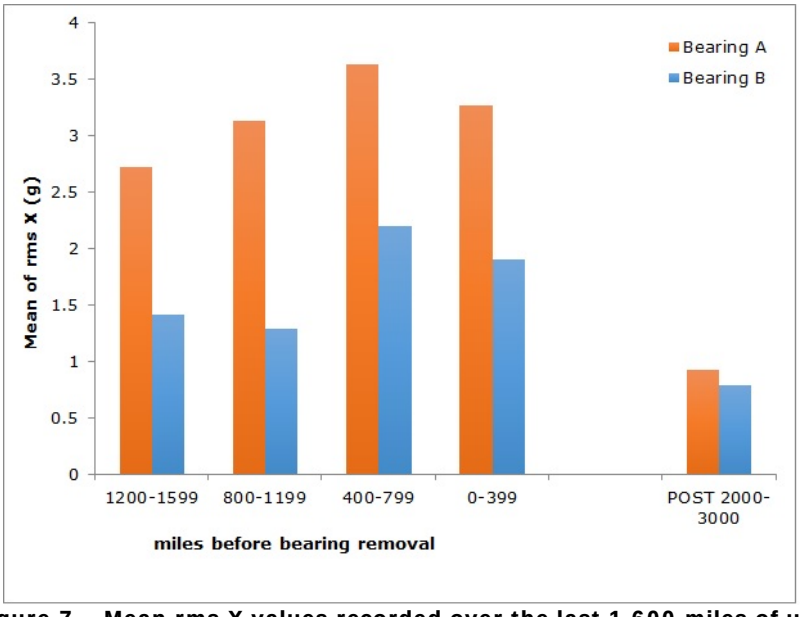

Figure 7 – Mean rms X values recorded over the last 1,600 miles of use before removal of each bearing. The values from bearing A are significantly higher than those for bearing B.

4.3 Outer race damage

Figure 8 shows the damaged outer races of the two bearings removed after the increase in vibrations shown in Figure 6. The damage observed has clear signs of rolling contact fatigue; more details are reported in (29). These two bearings will be used for this preliminary study to show the issues involved in linking vibration data to bearing damage. Bearing A shows 56 mm (36°) of uniform circumferential damage while bearing B shows a smaller damage over only 22 mm (14°). For every revolution of the train wheel 23 tapered rollers pass over the damage. The roller spacing of 15.65° suggests that only one roller was over the damage on bearing B, but two on bearing A. The damage on the outer race of bearing B is in two separate areas as if the two damages have been initiated separately. The damage observed in these bearings is similar to those reported in other studies (34, 36-37).

a)

b)

Figure 8 – Examples of damage on the outer race for a) bearing A and b) bearing B.

4.4 Surface profilometry of failed bearings

Table 1 - Damage for bearings A and B.

Variable	Bearing A	Bearing B	Ratio A:B
Damage arc (°)	35.82	14.39	2.5 : 1
Damage depth (average of 20 and 30 mm) (mm)	0.77	0.34	2.3 :1
Area loss (average of 20 and 30 mm) (mm^2)	23.69	3.43	7 : 1
Volume loss (mm^3)	900	75	12 : 1

The surface profiles of the rolling area of the outer race for bearing A and B are shown in Figure 9; for bearing A only one trace is reported because the damage is similar across the outer race. Table 1 clearly shows that the damage in bearing A is bigger than that in bearing B with the damage width and depth being more than double and the volume loss being almost 12 times larger.

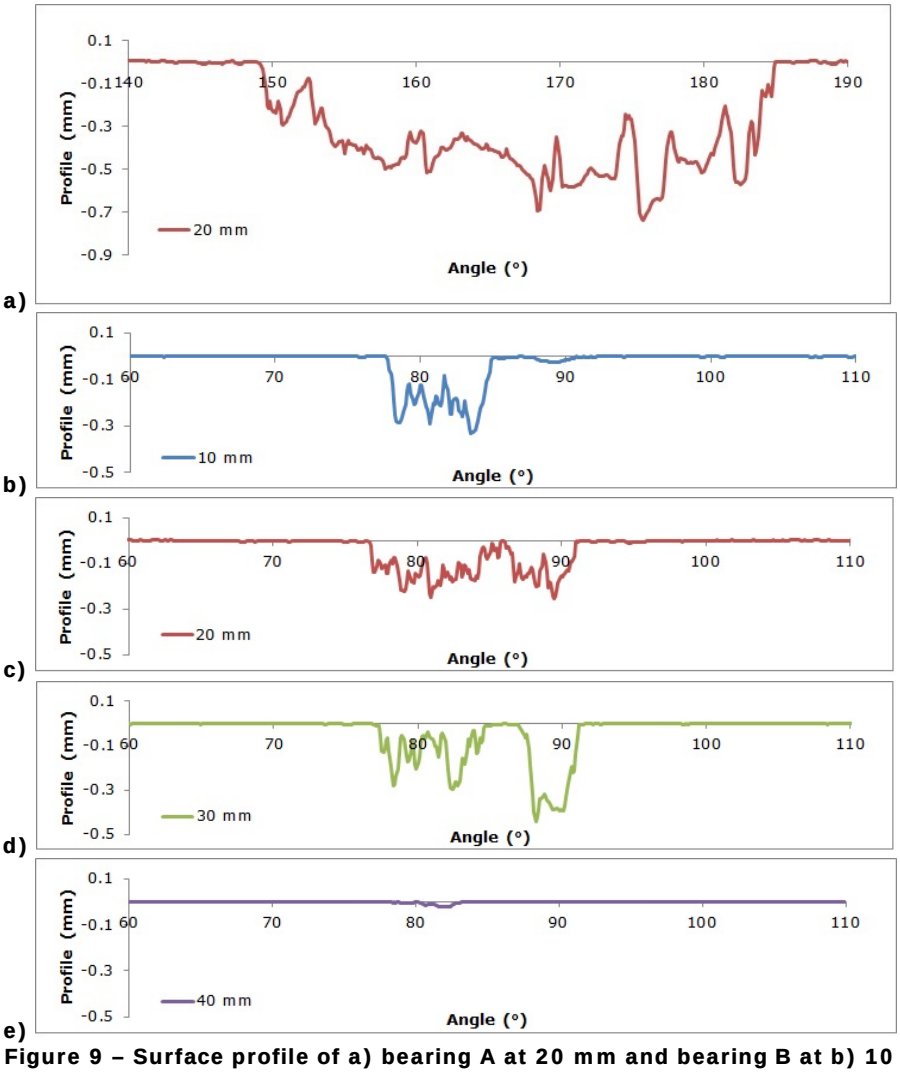

Figure 9 – Surface profile of a) bearing A at 20 mm and bearing B at b) 10 mm, c) 20 mm, d) 30 mm and e) 40 mm.

4.5 Correlation between damage and vibrations measured

From the two examples presented above, it seems that the extent of damage is comparable to the increase in vibrations. There is a loose proportionality that suggests that a bearing with twice the damage size will produce a doubling in the vibration amplitude. However, the bearing described in (29) (damage arc = 60°, damage depth = 0.8 mm, volume loss = 1,245 mm^3, rms X = 5) does not fit this pattern. More examples of bearings are needed to be able to understand this very complex system.

This two-bearing model is very simplistic, it has been observed that the measured vibrations grow with different slopes: 4 g in 11 days (bearing A) and 2 g in 48 days (bearing B) (Figure 6); indicating that other parameters are affecting the damage growth and in turn the vibrations measured. The loading profile is not considered to be a variable affecting these behavioural differences as both trains were proven to be subjected to the same conditions.

However, the following variables could influence the vibration/damage correlation:

- metallurgical differences (i.e. a bearing with a large subsurface flaw may present a unique damage/vibration pattern),
- isolated loading events that have not been captured or have been filtered out,
- history of the bearing before the WSN was fitted,
- physical growth of the damage (e.g. the shape, depth and number of RCF macropits could influence the vibration signature as could also the subsequent smoothing of the fracture surface).

5 CONCLUSIONS

- It has been shown that the vibrations present at a wheel axle bearing are very complex and influenced by many factors. Even a "good" bearing will produce a spread of vibration data in all three axes (Figure 4).

- Limiting this study to rms X and filtering the data to those collected while travelling on a length of straight track allow comparison of the vibrations of two damaged bearings (Figure 7).

- With further evaluation of more real-life train axle bearings, it is hoped that a relationship may be found linking bearing damage to vibrations, further improving the accuracy of condition monitoring and ultimately the safety of the train.

ACKNOWLEDGEMENTS

The authors gratefully acknowledge the EPSRC IAA funding, Dr Liam Goodes for measuring the volume loss and the Southeastern staff for their support.

REFERENCES

1. Gao, R. X., Jin, Y., Warrington, R. O. (1994) IEEE Transactions on instrumentation and measurement **43**, 216-219
2. Lei, Y., Lin, J., He, Z., Zuo, M. J. (2013) Mechanical Systems and Signal Processing **35**, 108–126 C
3. Lacey, S. J. (2008) Analysis, maintenance & asset management **23**, 32-42
4. Li, H., Zhang, Y., Zheng, H. (2010) Journal of Mechanical Science and Technology **23**, 291–301. doi:10.1007/s12206-008-1110-5
5. Li, H., Fu, L., Zheng, H. (2011) Journal of Mechanical Science and Technology **25**, 2731-2740
6. Ming, A. B., Qin, Z. Y., Zhang, W., Chu, F. L. (2013) Mechanical Systems and Signal Processing **41**, 141–154
7. Georgoulas, G., Loutas, T., Stylios, C. D., Kostopoulos, V. (2013) Mechanical Systems and Signal Processing **41**, 510–525
8. Feng, Z., Zuo, M. J., Hao, R., Chu, F., Lee, J. (2013) J. Vib. Acoust. **135**, 031013 1-21

9. Cocconcelli, M., Bassi, L., Secchi, C., Fantuzzi, C., Rubini, R. (2012) Mechanical Systems and Signal Processing **27**, 667–682
10. Tsao, W-C., Li, Y-F., Le, D. D., Pan, M-C. (2012) Measurement **45**, 1489–1498
11. Mohammadi, A., Safizadeh, M. S. (2013) Journal of Tribology **135**, 011102-1
12. Lei, Y., Lin, J., He, Z., Zi, Y. (2011) Mechanical Systems and Signal Processing **25**, 1738–1749
13. Wang, D., Tse, P. W., Tsui, K. L. (2013) Mechanical Systems and Signal Processing **35**, 176–199
14. Kar, C., Mohanty, A. R. (2004) Journal of Sound and Vibration **269**, 439–454
15. Mba, D., Rao, R. B. K. N. (2006) The shock and vibration digest **38**, 3-16
16. Elforjani, M., Mba, D. (2010) Engineering Fracture Mechanics **77**, 112–127
17. Jiang, R., Chen, J., Dong, G., Liu, T., Xiao, W. (2013) Proceedings of the Institution of Mechanical Engineers, Part C: Journal of Mechanical Engineering Science **227**, 1116-1129
18. Dybała, J., Zimroz, R. (2014) Applied Acoustics **77**, 195–203
19. Jiang, F., Zhu, Z., Li, W., Chen, G., Zhou, G. (2014) Meas. Sci. Technol. **25**, 025003
20. Yan, R., Gao, R. X., Chen, X. (2014) Signal Processing **96**, 1–15
21. Zhu, D., Gao, Q., Sun, D., Lu, Y., Peng, S. (2014) Signal Processing **96**, 80–89
22. Yu, G., Li, C., Zhang, J. (2013) Mechanical Systems and Signal Processing **41**, 155–175
23. Yang, W., Court, R. (2013) Measurement **46**, 2781–2791
24. Zhao, M., Jin, X., Zhang, Z., Li, B. (2014) Expert Systems with Applications **41**, 3391–3401
25. Symonds, N. (2004) Control and Reduction of Wear in Military Platforms NATO AVT-109, Williamsburg, US
26. Symonds, N. (2005) Insight - Non-Destructive Testing and Condition Monitoring **47**, 472-477
27. Zakrajsek, J. J., Dempsey, P. J., Huff, E. M., Augustin, M., Safa-Bakhsh, R., Duke, A., Ephraim, P., Grabil, P., Decker, H. J. (2006) Technical Report No. NASA/TM-2006- 214022
28. Trilla, A., Gratacòs, P. (2013) Chemical Engineering Transactions **33**, 733-738
29. Symonds, N., Corni, I., Wood, R. J. K., Wasenczuk, A., Vincent, D. ICEFA VI, manuscript in preparation
30. Zhao, J-S., Liu, W., Zhanga, Y., Feng, Z-J., Ye, J., Niu, Q-B. (2013) Mechanism and Machine Theory **69**, 185–199
31. Rosado, L., Forster, N. H., Thompson, K. L., Cooke, J. W. (2009) Tribology Transactions **53**, 29-41
32. Arakere, N. K., Branch, N., Levesque, G., Svendsen, V., Forster, N. H. (2009) Tribology Transactions **53**, 42-51
33. Forster, N. H., Rosado, L., Ogden, W. P., Trivedi, H. T. (2009) Tribology Transactions **53**, 52-59
34. Tsukahara, H., Aime, W., Burle, A., Chavance, D., Mouille, E. (2013) World Congress on Railway Research
35. Kalay, S., French, P., Tournay, H. (2011) World Congress of Railway Research
36. SKF, Railway technical handbook Volume 2 (2012) ISBN 978-91-978966-6-5
37. Müller, L., Sunder, R. (2013) World Congress on Railway Research
38. Bellaj, S., Pouzet, A., Mellet, C., Vionnet, R., Chavance, D. (2011) World Congress of Railway Research